Insights on the cuprate high energy anomaly observed in ARPES

B. Moritz[a,b,1,*], S. Johnston[a,c], T. P. Devereaux[a,d]

[a] *Stanford Institute for Materials and Energy Science, SLAC National Accelerator Laboratory, Menlo Park, CA 94025, USA*
[b] *Department of Physics and Astrophysics, University of North Dakota, Grand Forks, ND 58202, USA*
[c] *Department of Physics and Astronomy, University of Waterloo, Waterloo, ON N2L 3G1, Canada*
[d] *Geballe Laboratory for Advanced Materials, Stanford University, Stanford, CA 94305, USA*

Abstract

Recently, angle-resolved photoemission spectroscopy has been used to highlight an anomalously large band renormalization at high binding energies in cuprate superconductors: the high energy "waterfall" or high energy anomaly (HEA). The anomaly is present for both hole- and electron-doped cuprates as well as the half-filled parent insulators with different energy scales arising on either side of the phase diagram. While photoemission matrix elements clearly play a role in changing the aesthetic appearance of the band dispersion, *i.e.* creating a "waterfall"-like appearance, they provide an inadequate description for the physics that underlies the strong band renormalization giving rise to the HEA. Model calculations of the single-band Hubbard Hamiltonian showcase the role played by correlations in the formation of the HEA and uncover significant differences in the HEA energy scale for hole- and electron-doped cuprates. In addition, this approach properly captures the transfer of spectral weight accompanying doping in a correlated material and provides a unifying description of the HEA across both sides of the cuprate phase diagram. We find that the anomaly demarcates a transition, or cross-over, from a quasiparticle band at low binding energies near the Fermi level to valence bands at higher binding energy, assumed to be of strong oxygen character.

Keywords: ARPES, quantum Monte Carlo, Hubbard, strong correlations
PACS: 74.72.-h, 79.60.-i, 74.25.Jb, 71.10.Fd

Advancements in angle-resolved photoemission spectroscopy, an important probe of electronic structure, [1] have impacted significantly the study of strongly correlated materials. High resolution experiments, at binding energies up to 1 eV and higher, made possible by these advances, have revealed the presence of a "waterfall"-like structure with a characteristic kink at intermediate binding energies – the high energy anomaly (HEA) – in the dispersion of high T_c superconductors. [2–12] Found universally in hole-doped compounds, the characteristic HEA energy scale is ~ 300 meV with similar a dispersion anomaly observed in the half-filled parent insulators. [13] In contrast to earlier low energy studies focusing on dispersion kinks under ~ 100 meV, [14] interpreted as signatures of coupling to low energy bosonic modes, [15–17] the extrapolated band bottom has a value larger than that obtained from band structure calculations [2, 3] and the energy scale associated with the anomaly would tend to rule-out coupling to similar bosonic modes as the origin of the HEA.

More recently, anomalies have been found in electron-doped compounds at approximately twice the energy scale. [9–12] Taken together with results from hole-doped and half-filled parent materials, these findings raise questions about the origin or mechanism of the HEA, given the apparent dichotomy in energy scales between electron- and hole-doped compounds, and what role, if any, many body effects may play. Focusing primarily on the HEA in hole-doped compounds, a number of theories have been advanced including spin-charge separation, [3] in-gap band-tails, [18] spin polarons, [19] coupling to spin fluctuations, [6, 20, 21] phonons, [4] or plasmons, [22] strong correlation or "Mott" physics, [2, 23–26] and even extrinsic effects associated with photoemission matrix elements. [7]

Photoemission matrix elements clearly play a role in modifying the appearance of the HEA, complicating the analysis. The kink- or "waterfall"-like structure found in the first Brillouin zone (BZ) in experiments performed using synchrotron sources appears instead in newer experiments performed using low photon energy, laser sources as a band "break-up" or cross-over between a shallow, dispersing band crossing the Fermi level and a higher binding energy feature near the Γ-point. [8] Matrix element effects also influence the results of investigations in higher BZs which find a shallow band with a characteristic "Y" appearance near the zone center, rather than a true "waterfall". [7] However, the shallow, dispersing band near the Fermi level, together with the cross-over at the HEA energy scale seen in both hole- and electron-doped cuprates, [8, 11, 12] originates from intrinsic band renormalization effects and not extrinsic mechanisms that merely serve to

*Corresponding author
[1] E-mail address: moritzb@slac.stanford.edu

change the appearance of features with changing experimental conditions. [27] Those theoretical scenarios based on weak coupling to high energy bosonic modes [4, 6, 20–22, 27] have an appeal based on the kink-like appearance of the HEA, recalling earlier efforts aimed at explaining the origin of the low-energy kink in cuprates. [14–17] However, coupling to these modes, such as spin fluctuations, which would generally satisfy the energy scale for the HEA in hole-doped compounds, fails to account for the dichotomy in energy scales between hole- and electron-doped materials. However, spin fluctuations should play a prominent role in the renormalization mechanism forming the shallow, dispersing quasiparticle band for either hole- or electron-doped systems.

To investigate the influence that many-body effects, *i.e.* strong correlations, may have on the origin of the HEA we investigate the single-particle spectral function of the single-band Hubbard model, building upon and adding to the information obtained from much earlier investigations. [28–30] Using quantum Monte Carlo [31, 32] and the maximum entropy method (MEM) for analytic continuation, [33, 34] we study the spectral function for various values of electron filling. Our results indicate that the HEA can be connected to doping and the accompanying transfer of spectral weight into the lower or upper Hubbard band (LHB or UHB) of hole- or electron-doped systems, respectively. Doping leads to the formation of a quasiparticle band (QPB) at energies near the Fermi level, here set equal to zero energy, and the HEA represents a crossover from this band to the LHB, playing the role of valence bands in the cuprates that would have substantial oxygen character. Correlations and spectral weight transfers in the model lead to a natural asymmetry in the HEA energy scale between hole and electron doping, in agreement with experiment. The results also show qualitative similarities between the momentum dependence of the HEA from model calculations and that found experimentally.

The single-band Hubbard Hamiltonian, an effective, low energy model for the cuprates derived from downfolding multi-orbital models explicitly incorporating copper and oxygen degrees of freedom, [35, 36] has the form

$$H = -\sum_{ij,\sigma} t_{ij} c^{\dagger}_{i,\sigma} c_{j,\sigma} - \mu \sum_{i,\sigma} n_{i,\sigma} + \sum_{i} U (n_{i,\uparrow} - \frac{1}{2})(n_{i,\downarrow} - \frac{1}{2}),$$

where $c^{\dagger}_{i,\sigma}(c_{i,\sigma})$ creates (annihilates) an electron with spin σ at site i, the site occupation $n_{i,\sigma} = c^{\dagger}_{i,\sigma} c_{i,\sigma}$ for each spin species equals 0 or 1, $\{t_{ij}\}$ is a set of tight-binding coefficients parameterizing the electron kinetic energy (in this study we restrict ourselves to nearest-neighbor, t, and next-nearest-neighbor, t', terms), the chemical potential μ controls the electron filling, and the Hubbard repulsion U controls the strength of electron-electron correlations. The model is studied using determinant quantum Monte Carlo, [31, 32] an auxiliary-field technique. This method yields the finite temperature, imaginary time propagator $G_{ij}(\tau)$ on a finite-size cluster with periodic boundary conditions.

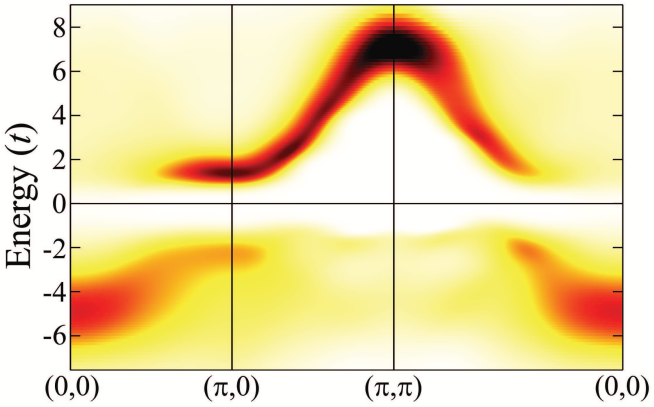

Figure 1: Bandstructure of the undoped single-band Hubbard model along high symmetry directions in the BZ. Model parameters: $t' = -0.30t$, $\mu = 0.00t$, $U = 8.00t$. The UHB has a pronounced dispersion along the $(\pi, 0) - (\pi, \pi)$ and $(0, 0) - (\pi, \pi)$ directions. The LHB, broad and centered at the Γ-point, has similar dispersing features, better separated from the bulk of the LHB especially along the $(0, 0) - (\pi, \pi)$ direction. Note the well separated intensity near $(\pi/2, \pi/2)$ between $-1t$ and $-2t$ and that at $(\pi, 0)$ near $-2t$. These dispersing features are precursors to the QPB that forms upon electron or hole doping. (Color online)

Estimates for this propagator in imaginary time come from individual Markov chains of the Monte Carlo process. This imaginary time propagator must be Wick rotated, or analytically continued, to real frequencies to extract the spectral function. Performing a discrete Fourier transform and treating the ensemble $\{G_K(\tau)\}$ obtained from individual Markov chains as a statistical sampling of the finite temperature propagator, the MEM, [33, 34] based on Bayesian inference, is used to obtain the single-particle spectral function $A(\mathbf{K}, \omega)$ on the appropriate discrete momentum grid.

The finite-size, square clusters used in this study have linear dimension $N = 8$ (64-site clusters). The corresponding momentum space grid $\{K\}$ has a point spacing of $\pi/4$. The imaginary time interval, partitioned into L "slices" of size $\Delta\tau = \beta/L$, runs from 0 to $\beta = 1/T$, the inverse temperature, and t serves as the energy unit of the problem. In this study, $\beta = 3/t$ and $\Delta\tau = 1/16\,t$. Once $A(\mathbf{K}, \omega)$ has been obtained on the discrete momentum grid, the single-particle self-energy $\Sigma(\mathbf{K}, \omega)$ can be extracted using Dyson's equation and the bare bandstructure corresponding to the tight-binding, model parameters. Assuming a weak momentum dependence to the self-energy, an interpolation routine provides the value of $\Sigma(\mathbf{k}, \omega)$ at an arbitrary point $\mathbf{k}$ in the BZ and Dyson's equation can be employed to compute $A(\mathbf{k}, \omega)$.

Figure 1 shows the bandstructure along high symmetry directions in the BZ for the undoped single-band Hubbard model with parameters $t' = -0.30t$, $\mu = 0.00t$, and $U = 8.00t$. At the Γ-point and (π, π) one finds the bulk of the incoherent LHB and UHB, respectively. Above the Fermi level, the UHB has dispersing branches along the $(\pi, 0) - (\pi, \pi)$ and $(0, 0) - (\pi, \pi)$ directions with signifi-

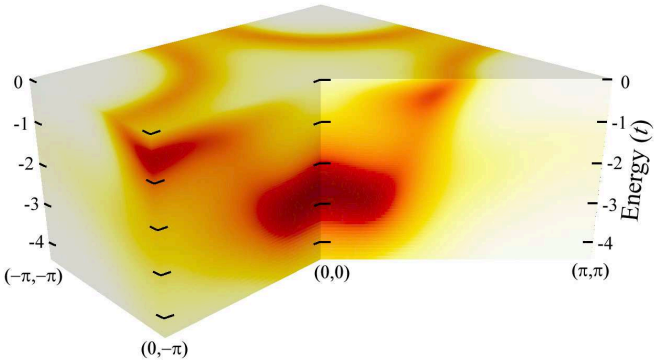

Figure 2: Bandstucture of the hole-doped ($\sim 14\%$) single-band Hubbard model along high symmetry directions in the BZ below the Fermi level. Each face represents a different symmetry direction arranged in the proper geometric relationship to one another. The top face shows the Fermi surface with a portion removed, exposing the bandstructure along the BZ axis (the $(0,0)-(0,-\pi)$ direction) and BZ diagonal (the $(0,0)-(\pi,\pi)$ direction). Model parameters: $t' = -0.30t$, $\mu = -2.50t$, $U = 8.00t$. In this figure, the spectral function $A(\mathbf{k},\omega)$ has been multiplied by the Fermi distribution function $f(\omega)$. The dispersing QPB crosses the Fermi level and remains shallow, at low binding energies, giving way to the LHB, localized near the Γ-point, with a cross-over of weaker intensity at intermediate binding energies. (Color online)

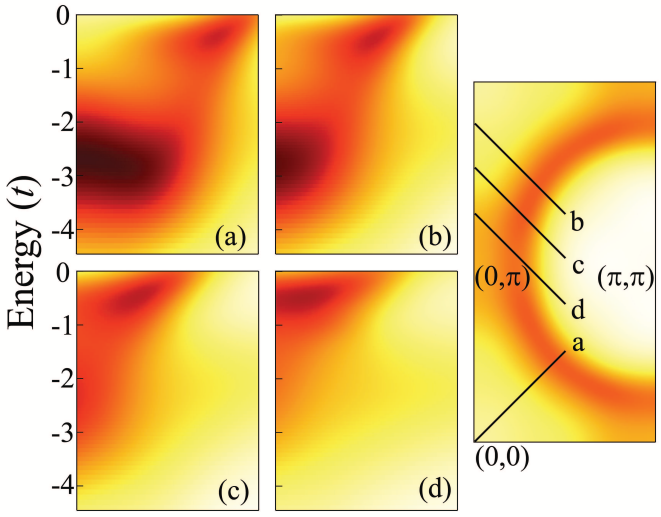

Figure 3: Momentum dependence of the hole-doped spectral function multiplied by the Fermi distribution function along selected cuts in the BZ. Model parameters: $t' = -0.30t$, $\mu = -2.50t$, $U = 8.00t$. Panels (a)-(d) show the intensity (falsecolor scale) along the cuts highlighted in the right panel. This sequence of cuts highlights the distinction between the QPB and the LHB and shows the evolution of the "waterfall"-like appearance of the HEA moving along the BZ axis away from the Γ-point. (Color online)

cant spectral weight in the region near $(\pi, 0)$. Below the Fermi level, the bulk of the LHB spectral weight is concentrated near the Γ-point; however, there is less pronounced, but better separated, dispersing spectral weight along the $(0,0)-(\pi,0)$ and $(0,0)-(\pi,\pi)$ directions.

There is a significant spectral weight in this dispersing feature near $(\pi/2, \pi/2)$ between $-1t$ and $-2t$ before losing intensity upon approaching the Γ-point and the bulk of the LHB. A similar energy scale can be assigned to the dispersing feature near $(\pi, 0)$. The behavior of the spectral intensity along the $(0,0)-(\pi,\pi)$ direction is qualitatively similar to that observed in experiment [13] with a low binding energy feature near $(\pi/2, \pi/2)$ crossing-over to the valence band at the Γ-point with the transition marked by the appearance of a "waterfall" at intermediate binding energies. These dispersing features are precursors to the QPB that appears upon electron or hole doping.

Figure 2 shows the bandstructure for the hole-doped single-band Hubbard model below the Fermi level along high symmetry directions in the BZ, arranged with the appropriate geometrical relationship. Here the spectral function has been multiplied by the Fermi distribution function $f(\omega) = (\exp(\beta\omega) + 1)^{-1}$. The incoherent LHB, effectively localized near the Γ-point, has a weak tail of intensity extending toward the points (π, π) and $(0, -\pi)$. The decrease in intensity within these tails approximately coincides with the location in momentum space identified with the HEA.

Along the $(0,0)-(\pi,\pi)$ direction, the QPB disperses across the Fermi level at $\sim (\pi/2, \pi/2)$. Near $(\pi/4, \pi/4)$ the spectral intensity drops and the HEA appears as an apparent cross-over from the QPB to the LHB at an energy $\sim -0.5t$ to $-0.75t$, the HEA energy scale. Along the $(0,0)-(0,-\pi)$ direction, the QPB is nearly non-dispersive at an energy $\sim -0.5t$. At approximately $(0, -\pi/2)$ the QPB crosses-over to the LHB with a weak tail of intensity at low binding energy extending toward the Γ-point. While the spectral intensity decreases in the QPB approaching the Γ-point, there is significant coexistence of the LHB and QPB as a function of momentum along these high symmetry cuts. The spectral function has a "waterfall"-like appearance even without including the effect of photoemission matrix elements, which serve to enhance the appearance by further suppressing intensity nearing the Γ-point. [11]

The relationship between the QPB, the LHB, and the appearance of the HEA can be further explored studying the detailed momentum dependence of the spectral function. Figure 3 shows the spectral function along selected momentum space cuts. Cut (a) reproduces a part of the spectral function along the $(0,0)-(\pi,\pi)$ direction already encountered in Fig. 2. Cuts (b)-(d) show the spectral function in momentum space, parallel to the $(0,0)-(\pi,\pi)$ direction, moving toward $(0,\pi)$. While the energy scale of the LHB remains relatively unchanged, its spectral intensity progressively decreases. The QPB, crossing the Fermi level, increasingly becomes easier to identify as a proper band with increased spectral weight approaching the BZ axis. The "waterfall"-like appearance of the HEA also evolves with changes to its momentum space position and progressive reduction in spectral intensity below the QPB. Taken as a whole, the evolution of the QPB and HEA qualitatively agree with the results of experiment on hole-doped compounds, [2, 3] including the evolution of

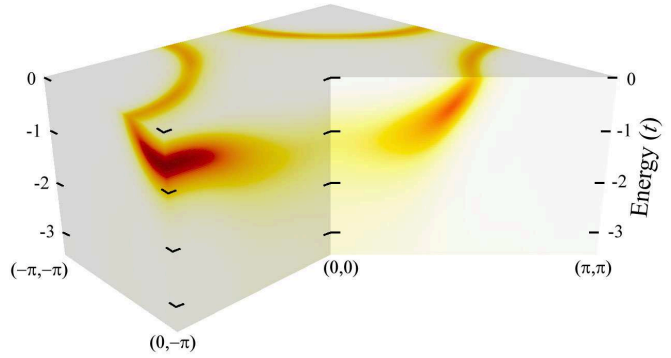

Figure 4: Bandstucture of the electron-doped ($\sim 17\%$) single-band Hubbard model along high symmetry directions in the BZ below the Fermi level. The top face shows the Fermi surface with a portion removed. Model parameters: $t' = -0.25t$, $\mu = 2.20t$, $U = 8.00t$. In this figure, the spectral function $A(\mathbf{k}, \omega)$ has been multiplied by the Fermi distribution function $f(\omega)$. The dispersing QPB crosses the Fermi level and remains shallow, at low binding energies approaching the Γ-point with diminishing intensity. The LHB (not shown) at higher binding energies ($\sim -7.5t$) has a substantially reduced intensity due to spectral weight transfer into the QPB and UHB with electron doping. The HEA energy scale is $\sim -1.0t$ to $-1.5t$, twice that found in the hole-doped system. (Color online)

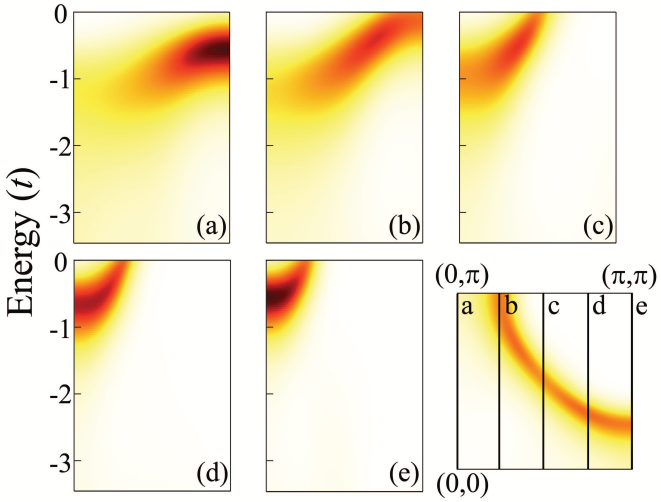

Figure 5: Momentum dependence of the electron-doped spectral function multiplied by the Fermi distribution function along selected cuts in the BZ. Model parameters: $t' = -0.25t$, $\mu = 2.20t$, $U = 8.00t$. Panels (a)-(e) show the intensity (falsecolor scale) along the cuts highlighted in the lower right panel. The lack of significant spectral intensity in the LHB suppresses the "waterfall"-like appearance of the HEA. (Color online)

spectral intensity and changes in momentum space position and robustness of the "waterfall"-like appearance as a function of momentum.

Comparison of calculation results for a hole-doped system to those for an electron-doped system reveal the dichotomy in HEA energy scales intrinsic to the single-band Hubbard model. Figure 4 shows the spectral function multiplied by the Fermi distribution function for an electron-doped system with model parameters $t' = -0.25t$, $\mu = 2.20t$, and $U = 8.00t$. The LHB (not shown) has a dramatically reduced intensity due to spectral weight transfers into the QPB and UHB upon electron doping. This affects the "waterfall"-like appearance of the HEA in the electron-doped calculation by reducing the spectral intensity at intermediate binding energies between the QPB and the LHB. Previous results demonstrate that modifying the spectral intensity through the inclusion of approximate matrix elements leads to enhanced "waterfall"-like character in the electron-doped dispersion. [11] For real-world experiments, the proper valence band, composed of significant oxygen character, should remain robust under electron-doping, increasing the likelihood of a prominent "waterfall"-like appearance in the cross-over region at intermediate binding energies, in agreement with experiment. [9–12]

The dispersive QPB shown in Fig. 4 dips farther below the Fermi level than does its hole-doped counterpart, yielding an HEA energy scale $\sim -1.0t$ to $-1.5t$ along the $(0,0) - (\pi,\pi)$ direction. Along the $(0,0) - (0,-\pi)$ direction, the spectral function appears to be quite similar to its hole-doped counterpart with an energy scale $\sim -0.5t$ near $(0,-\pi)$ with a weak dispersion in this region. Together with decreasing intensity, the QPB along this direction disperses downward to and energy $\sim -1.5t$ at the Γ-point. The chief contrast between the QPB in hole- and electron-doped systems, other than the energy scale, lies in their origin. With hole doping, the chemical potential moves down into the LHB, or more precisely the dispersive features at lower binding energy, and the QPB originates from the dispersive precursors shown in Fig. 1; whereas in electron-doped systems, the chemical potential shifts in the opposite direction and the QPB arises from the precursors in the UHB.

Figure 5 shows the momentum dependence of the QPB along selected cuts in the BZ. Like the hole-doped system, the spectral intensity near the BZ axis progressively increases moving from the Γ-point toward $(\pi, 0)$ or $(0, \pi)$. While there is significantly less intensity below the QPB compared with the hole-doped system, one can also infer changes to the HEA momentum space position and its "waterfall"-like appearance from cuts (a)-(e) that would be qualitatively similar to the hole-doped system. The most noticeable contrast to the hole-doped system is the change in the HEA energy scale between cuts (a) and (e), a factor on the order of 2 or 3, seen directly in the cut along the BZ axis (cut (a) of Fig. 5). As in the hole-doped case, these results qualitatively capture the behavior observed in experiments on electron-doped compounds. [12]

The results presented in this study provide evidence for an HEA in the single-band Hubbard model. The findings appear to agree qualitatively (quantitatively with a proper choice for the energy scale t) with experiments on both hole- and electron-doped compounds as well as the half-filled parent insulators. In principle, the results would include effects associated with the coupling of electrons to

spin fluctuations, one of the theoretical scenarios for the origin of the HEA, at an energy scale proportional to the superexchange constant J that should have a similar value in hole- and electron-systems. However, the dichotomy in the HEA energy scale between hole- and electron-doped systems (a factor of ~ 2) would argue against solely this origin due to bosonic-mode coupling. Instead these results support the conclusion that strong correlations play a central role in the origin of the HEA and that the anomaly itself results from a simple cross-over between the shallow, dispersing QPB near the Fermi level and the incoherent LHB at higher binding energy.

The authors would like to thank R. Hackl, M. Jarrell, C. Kim, W. S. Lee, A. Macridin, T. Maier, W. Meevasana, R. T. Scalettar, F. Schmitt, Z.-X. Shen, and F. Vernay for valuable discussions. This work is supported in part by the U.S. Department of Energy, Office of Basic Energy Sciences, Division of Materials Sciences and Engineering, under contract DOE DE-AC02-76SF00515. SJ would like to acknowledge support from NSERC and SHARCNET. This work was made possible, in part, by computational support from the National Energy Research Scientific Computing Center, which is supported by the Office of Science of the U.S. Department of Energy under Contract No. DE-AC02-05CH11231, NSF through TeraGrid resources provided by the National Center for Supercomputing Applications, Réseau Québécois de Calcul de Haute Performance through Mammouth-parallèle at the University of Sherbrooke and the facilities of SHARCNET. The authors wish to thank the Walther Meißner Institute and the Pacific Institute of Theoretical Physics for their hospitality during part of this work.

[1] A. Damascelli, Z. Hussain, Z.-X. Shen, Rev. Mod. Phys. 75 (2003) 473.
[2] W. Meevasana, X. J. Zhou, S. Sahrakorpi, W. S. Lee, W. L. Yang, K. Tanaka, N. Mannella, T. Yoshida, D. H. Lu, Y. L. Chen, R. H. He, H. Lin, S. Komiya, Y. Ando, F. Zhou, W. X. Ti, J. W. Xiong, Z. X. Zhao, T. Sasagawa, T. Kakeshita, K. Fujita, S. Uchida, H. Eisaki, A. Fujimori, Z. Hussain, R. S. Markiewicz, A. Bansil, N. Nagaosa, J. Zaanen, T. P. Devereaux, Z.-X. Shen, Phys. Rev. B 75 (2007) 174506.
[3] J. Graf, G.-H. Gweon, K. McElroy, S. Y. Zhou, C. Jozwiak, E. Rotenberg, A. Bill, T. Sasagawa, H. Eisaki, S. Uchida, H. Takagi, D.-H. Lee, A. Lanzara, Phys. Rev. Lett. 98 (2007) 067004.
[4] B. P. Xie, K. Yang, D. W. Shen, J. F. Zhao, H. W. Ou, J. Wei, S. Y. Gu, M. Arita, S. Qiao, H. Namatame, M. Taniguchi, N. Kaneko, H. Eisaki, K. D. Tsuei, C. M. Cheng, I. Vobornik, J. Fujii, G. Rossi, Z. Q. Yang, D. L. Feng, Phys. Rev. Lett. 98 (2007) 147001.
[5] J. Chang, S. Pailhés, M. Shi, M. Månsson, T. Claesson, O. Tjernberg, J. Voigt, V. Perez, L. Patthey, N. Momono, M. Oda, M. Ido, A. Schnyder, C. Mudry, J. Mesot, Phys. Rev. B 75 (2007) 224508.
[6] T. Valla, T. E. Kidd, W.-G. Yin, G. D. Gu, P. D. Johnson, Z.-H. Pan, A. V. Fedorov, Phys. Rev. Lett. 98 (2007) 167003.
[7] D. S. Inosov, J. Fink, A. A. Kordyuk, S. V. Borisenko, V. B. Zabolotnyy, R. Schuster, M. Knupfer, B. Büchner, R. Follath, H. A. Dürr, W. Eberhardt, V. Hinkov, B. Keimer, H. Berger, Phys. Rev. Lett. 99 (2007) 237002.
[8] W. Zhang, G. Liu, J. Meng, L. Zhao, H. Liu, X. Dong, W. Lu, J. S. Wen, Z. J. Xu, G. D. Gu, T. Sasagawa, G. Wang, Y. Zhu, H. Zhang, Y. Zhou, X. Wang, Z. Zhao, C. Chen, Z. Xu, X. J. Zhou, Phys. Rev. Lett. 101 (2008) 017002.
[9] Z.-H. Pan, P. Richard, A. Fedorov, T. Kondo, T. Takeuchi, S. Li, P. Dai, G. Gu, W. Ku, Z. Wang, H. Ding, arXiv:cond-mat/0610442.
[10] S. R. Park, C. S. Leem, Y. S. Roh, K. J. Choi, J. H. Kim, B. J. Kim, H. Koh, H. Eisaki, D. H. Lu, Z.-X. Shen, N. Armitage, C. Kim, J. Phys. Chem. Sol. 69 (2008) 2939.
[11] B. Moritz, F. Schmitt, W. Meevasana, S. Johnston, E. M. Motoyama, M. Greven, D. H. Lu, C. Kim, R. T. Scalettar, Z.-X. Shen, T. P. Devereaux, New J. Phys. 11 (2009) 093020.
[12] M. Ikeda, T. Yoshida, A. Fujimori, M. Kubota, K. Ono, Y. Kaga, T. Sasagawa, H. Takagi, Phys. Rev. B 80 (2009) 184506.
[13] F. Ronning, K. M. Shen, N. P. Armitage, A. Damascelli, D. H. Lu, Z.-X. Shen, L. L. Miller, C. Kim, Phys. Rev. B 71 (2005) 094518.
[14] X. J. Zhou, T. Cuk, T. P. Devereaux, N. Nagaosa, Z.-X. Shen, in: J. R. Schrieffer, J. S. Brooks (Eds.), Handbook of High-Temperature Superconductivity: Theory and Experiment, Springer-Verlag, New York, 2007.
[15] T. P. Devereaux, T. Cuk, Z.-X. Shen, N. Nagaosa, Phys. Rev. Lett. 93 (2004) 117004.
[16] P. D. Johnson, T. Valla, A. V. Fedorov, Z. Yusof, B. O. Wells, Q. Li, A. R. Moodenbaugh, G. D. Gu, N. Koshizuka, C. Kendziora, S. Jian, D. G. Hinks, Phys. Rev. Lett. 87 (2001) 177007.
[17] A. Kaminski, M. Randeria, J. C. Campuzano, M. R. Norman, H. Fretwell, J. Mesot, T. Sato, T. Takahashi, K. Kadowaki, Phys. Rev. Lett. 86 (2001) 1070.
[18] A. S. Alexandrov, K. Reynolds, Phys. Rev. B 76 (2007) 132506.
[19] E. Manousakis, Phys. Rev. B 75 (2007) 035106.
[20] A. Macridin, M. Jarrell, T. Maier, D. J. Scalapino, Phys. Rev. Lett. 99 (2007) 237001.
[21] R. S. Markiewicz, S. Sahrakorpi, A. Bansil, Phys. Rev. B 76 (2007) 174514.
[22] R. S. Markiewicz, A. Bansil, Phys. Rev. B 75 (2007) 020508.
[23] K. Byczuk, M. Kollar, K. Held, Y.-F. Yang, I. A. Nekrasov, T. Pruschke, D. Vollhardt, Nature Phys. 3 (2007) 168.
[24] F. Tan, Y. Wan, Q.-H. Wang, Phys. Rev. B 76 (2007) 054505.
[25] M. M. Zemljič, P. Prelovšek, T. Tohyama, Phys. Rev. Lett. 100 (2008) 036402.
[26] C. Weber, K. Haule, G. Kotliar, Phys. Rev. B 78 (2008) 134519.
[27] S. Basak, T. Das, H. Lin, J. Nieminen, M. Lindroos, R. S. Markiewicz, A. Bansil, Phys. Rev. B 80 (2009) 214520.
[28] R. Preuss, W. Hanke, W. von der Linden, Phys. Rev. Lett. 75 (1995) 1344.
[29] C. Gröber, R. Eder, W. Hanke, Phys. Rev. B 62 (2000) 4336.
[30] E. Dagotto, Rev. Mod. Phys. 66 (1994) 763.
[31] S. R. White, D. J. Scalapino, R. L. Sugar, E. Y. Loh, J. E. Gubernatis, R. T. Scalettar, Phys. Rev. B 40 (1989) 506.
[32] R. Blankenbecler, D. J. Scalapino, R. L. Sugar, Phys. Rev. D 24 (1981) 2278.
[33] M. Jarrell, J. Gubernatis, Phys. Rep. 269 (3) (1996) 133.
[34] A. Macridin, S. P. Doluweera, M. Jarrell, T. Maier, arXiv:cond-mat/0410098v1.
[35] F. C. Zhang, T. M. Rice, Phys. Rev. B 37 (1988) 3759.
[36] P. W. Anderson, Science 235 (1987) 1196.